CHEMISTRY
AN ASIAN JOURNAL

DOI: 10.1002/asia.200800154

Glycan Arrays on Aluminum-Coated Glass Slides

Susan Y. Tseng,[a] Cheng-Chi Wang,[a, b] Chin-Wei Lin,[a] Cheng-Lung Chen,[c] Wen-Yueh Yu,[d] Chung-Hsuan Chen,[a] Chung-Yi Wu,*[a] and Chi-Huey Wong*[a]

Dedicated to Professor Ryoji Noyori on the occasion of his 70th birthday

Abstract: We have developed a novel method of immobilizing glycans onto aluminum-coated glass (ACG) slides for potential use in disease diagnosis and drug discovery. The quality of these sugar chips can be assessed by mass spectrometry and fluorescence measurements with high sensitivity. The unique properties of ACG slides include: 1) the metal oxide layer on the surface can be activated for grafting organic compounds such as modified oligosaccharides; 2) the surface remains electrically conductive, and the grafted oligosaccharides can be simultaneously characterized by mass spectrometry and carbohydrate-binding assay; and 3) the slides are more sensitive than transparent glass slides in binding analysis. To demonstrate this, we synthesized a model compound of mannose with a built-in photocleavable linker bound to the ACG slide surface. The molecular weight of the grafted mannose was identified by mass spectrometry, and the slide was subjected to biotinylated ConA binding followed by Cy3-tagged streptavidin detection. This method was further extended to the preparation of glycan arrays containing lactose and the cancer antigen Globo H.

Keywords: fluorescent probes · glycan arrays · mass spectrometry · microarrays · protein binding

Introduction

Carbohydrate microarrays are a powerful tool for the study of glycobiology and the high-throughput bioassay of epidemic diseases.[1] A fundamental problem of this technology is how to characterize and quantify the oligosaccharides that are covalently bound to the surface. Effective immobilization of sugars on the surface is essential for surviving consecutive substrate washing when evaluating sugar–protein binding. Mass spectrometry (MS) has been reported to be a useful analytical method[2] for the high-throughput characterization of immobilized sugars on porous glass slides.

Although a variety of substrates are commercially available for glycan arrays, they are not suitable for direct mass spectrometric analysis. These substrates include glass and polyethylene terephthalate (PET) coated with amine, carboxylate, *N*-hydroxysuccinimide (NHS), avidin, epoxy, aldehyde, chelating nickel groups, and so on. In fact, NHS-functionalized glass slides are commonly used[3,4] for the preparation of glycan arrays. A typical example is that of sugar antigens immobilized on the surface of the glass slide, after which a sugar-binding monoclonal antibody and a fluorescence-tagged secondary antibody were incubated for studies of protein–carbohydrate interaction. Although effective, these glass slides are not ideal for use to characterize the bound sugars by mass spectrometry.

Substrates selected for matrix-assisted laser desorption–ionization time-of-flight (MALDI-TOF) MS should be conductive or semiconductive so that a uniform electric field can be produced under high vacuum. Standard stainless-steel plates are usually the choice for loading the analytes.

[a] Dr. S. Y. Tseng, C.-C. Wang, C.-W. Lin, Dr. C.-H. Chen, Dr. C.-Y. Wu, Dr. C.-H. Wong
Genomics Research Center, Academia Sinica
128, Sec. 2, Academia Road
Nankang Dist., Taipei 11529 (Taiwan)
Fax: (+886) 2-2789-9931
E-mail: cyiwu@gate.sinica.edu.tw
chwong@gate.sinica.edu.tw

[b] C.-C. Wang
Institute of Biochemical Science
National Taiwan University
No. 1, Sec. 4, Roosevelt Road, Taipei 1061 (Taiwan)

[c] C.-L. Chen
Institute of Physics, Academia Sinica
128, Sec. 2, Academia Road
Nankang Dist. Taipei 11529 (Taiwan)

[d] W.-Y. Yu
Institute of Chemistry, Academia Sinica
128, Sec. 2, Academia Road
Nankang Dist. Taipei 11529 (Taiwan)

In MALDI MS, the energy of the pulse laser beam is absorbed by the matrix (miscible organic chemicals) to prevent sample fragmentation. MALDI-TOF MS is an excellent tool for analyzing high-molecular-weight biomolecules. However, the chemicals in the organic matrix interfere with low-molecular-weight oligosaccharides (typically less than 2000 Da); thus, porous silicon was chosen as the substrate for analyzing biomolecules by MS[2,5–7] without the addition of matrix chemicals. In desorption–ionization on silicon (DIOS) MS, biomolecules of relatively low molecular weight were identified on the basis of the m/z ratio of the pseudoparent peak from MS.

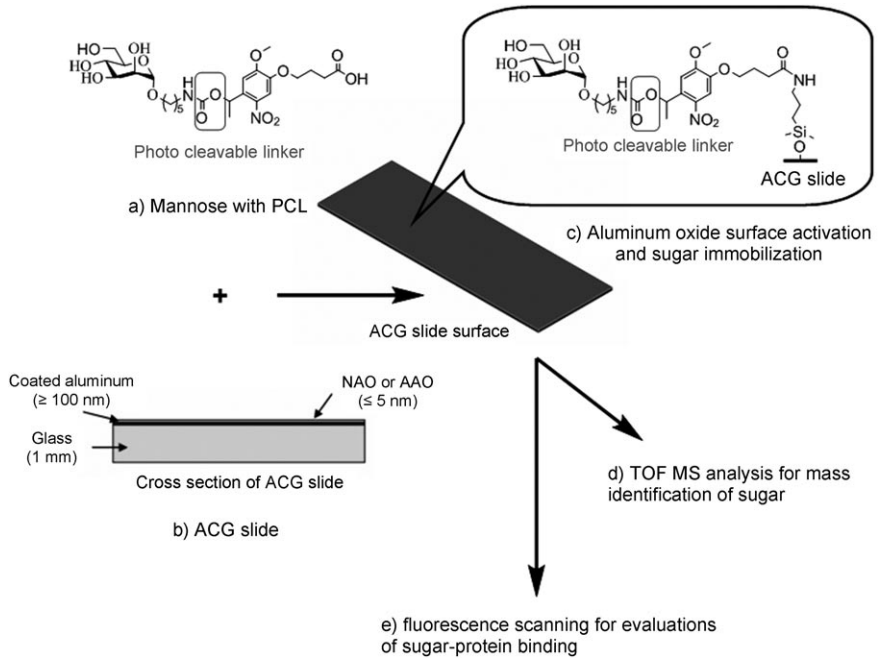

Scheme 1. a) A sugar derivative such as mannose with a built-in photocleavable linker. b) ACG slide ($75.5\times25.4\times1$ mm^3) with layers of aluminum oxide (<5 nm) on the surface and pure aluminum (>100 nm) coated on the glass slide (1 mm). c) The ACG slide was activated, and the sugar derivatives were immobilized (microarrayed and manually spotted) on the surface. The slide was subjected to d) molecular-weight identification of the sugar by mass spectrometry and e) further evaluated for its sugar–protein binding by a fluorescence scanner.

Effective adhesion between sugar molecules and the substrate surfaces have been achieved through covalent bonding.[1,2,8] Physical adsorption of sugar derivatives on fluorous surfaces[9] may also be feasible for sufficient adhesion. Porous silicon plates also acted as a matrix in DIOS MS, and mass spectra were obtained with a high signal-to-noise (S/N) ratio without fragmentation. The preparation of porous silicon plates requires the usage of corrosive acid, which is not environmentally friendly, and the quality of the plates is difficult to control. On the other hand, porous aluminum oxide exists naturally on the surface of aluminum; the electrochemical anodization of aluminum-coated glass (ACG) slides can be carried out in mildly acidic aqueous solution. Silylation reactions on silicon surfaces[10–12] can also be used on aluminum surfaces under proper conditions. The freshly cut surface of plate aluminum has a shiny metallic texture. When exposed to air, the surface gradually oxidizes and turns opaque as a layer of aluminum oxide (called native oxide) is formed. Native aluminum oxide (NAO) grown on aluminum surfaces has no orientation compared to that of anodized aluminum oxide (AAO). The thickness of NAO on aluminum surfaces is just a few nanometers.[12] In contrast, the thickness of AAO could grow quickly (within 15–20 min) to the micrometer range with the growing direction aligned to an applied electric field. In a few trial experiments, we fabricated pure aluminum plates (with a thickness of 1 mm) and deliberately grew the AAO layer to 2 μm on the surface of the plate. This surface with a thick layer of AAO became nonconductive (like ceramics) and was not suitable for our study. However, in all cases, the amorphous oxide layers on the aluminum surfaces could be modified chemically, and the substrate remained electrically conductive only when the thickness of the oxide layer on the surface was in the nanometer range.

In this study (Scheme 1), we fabricated several new substrates with a thin layer of aluminum oxide on the surface of ACG slides in an attempt to characterize the molecular weight of the surface-grafted oligosaccharide and simultaneously to look for its sugar–protein binding capability. Designed mannose and lactose derivatives with a built-in pho-

Abstract in Chinese:

此篇文獻報告鋁膜玻片表面與寡醣共價鍵結的特殊性質與應用：(1)鋁膜玻片表面的氧化層可以被活化，然後與有機物，例如修飾過的寡醣做共價鍵結。(2)鋁膜玻片的表面保持導電性，鍵結的寡醣可以質譜儀(MS-TOF)定訂寡醣的分子量也可以同時將寡醣在鋁膜玻片上微陣排列，與含有螢光的蛋白質做結合，經由螢光掃描分析寡醣與特定蛋白質之間的凝集能力。(3)由於螢光在鋁膜玻片做全反射，使得鋁膜玻片偵測螢光的敏感度高於一般玻片。我們以甘露醣在實驗室中合成修飾出可以紫外光可斷裂開的甘露醣衍生有機物，將此甘露醣衍生有機物鍵結在鋁膜玻片的表面，其中部份鍵結的甘露醣直接用質譜儀(Ultraflex MS-TOF)作甘露醣的分子量的定性。另外一部份鍵結的甘露醣與ConA/生物素做凝集再與含有螢光Cy3的streptavidin做二次凝集之後用螢光掃描儀(arrayWoRx)分析。以上的實驗發現質譜儀與螢光偵測儀所得到的數據之間有半定量的相關結果。氧化鋁的原子團與特殊如乳醣衍生物的質譜分析會有些許干擾。而以Globo H衍生物做類似測試，其螢光偵測敏感度確實較一般玻片高出許多。驗證了鋁膜玻片的特殊物性與其可應用性。

CHEMISTRY
AN ASIAN JOURNAL

tocleavable linker (PCL) were synthesized and covalently bound to the activated ACG slides (Scheme 2). Without addition of a miscible organic matrix, the sugar-immobilized ACG slides were subjected to molecular-weight identification and protein-binding evaluation.

Results and Discussion

Surface Properties of ACG Slides

A layer of pure aluminum (99.999%) at least 100 nm thick was coated onto the micro glass slides by using various coating techniques, such as magnetron sputtering, cathode arc evaporation, and thermal coating. These slides were either used without further manipulation or electrically anodized before usage. Figure 1 shows their surface morphology, composition, and roughness as determined by scanning electron microscopy (SEM), atomic force microscopy (AFM), and X-ray photoelectron spectroscopy (XPS). As can be seen, the ACG slide produced by cathode arc evaporation has a coating of large granules and a high surface roughness. Slides with high surface roughness affect the surface-wetting property. The magnetron-sputtered ACG slide gave an acceptable surface roughness; however, it required a long coating time to achieve the desired coating thickness and was used only at the early stages of this study.

As the study proceeded, we noticed that the thermally coated ACG slides achieved the desired coating thickness in a relatively short time. It gave the smoothest surface with a surface roughness of 10 nm. With subsequent surface-anodization treatment, the ACG slide provided a stable surface for grafting. Only the anodized slide surfaces were covered with 100% aluminum oxide (Figure 2).

The electrical resistance of the ACG slide (end-to-end distance) was measured between 1.6 and 4 Ω. These slides became electrically nonconductive when the oxide layer grew thick. The depth of penetration for XPS was 20–50 Å, and the thickness of the oxide layer (either NAO or AAO) in this study was estimated from the cross-section to be no more than 5 nm.

The thickness of coated aluminum on the glass slide needs to be >100 nm so that the substrate remains nontransparent within the visible region. When a transparent substrate was used, part of the fluorescent light passed through the substance, and the scanner detected only a portion of the Cy3 fluorescence. The instrument detected more fluorescent light when a nontransparent ACG slide was used as the background substrate. Figure 3 shows the optical properties of ACG slides compared to those of the micro glass slide. The thickness of the coated aluminum on the semitransparent ACG slides was just a few nanometers, and that of the reflective ACG slides was approximately 300 nm.

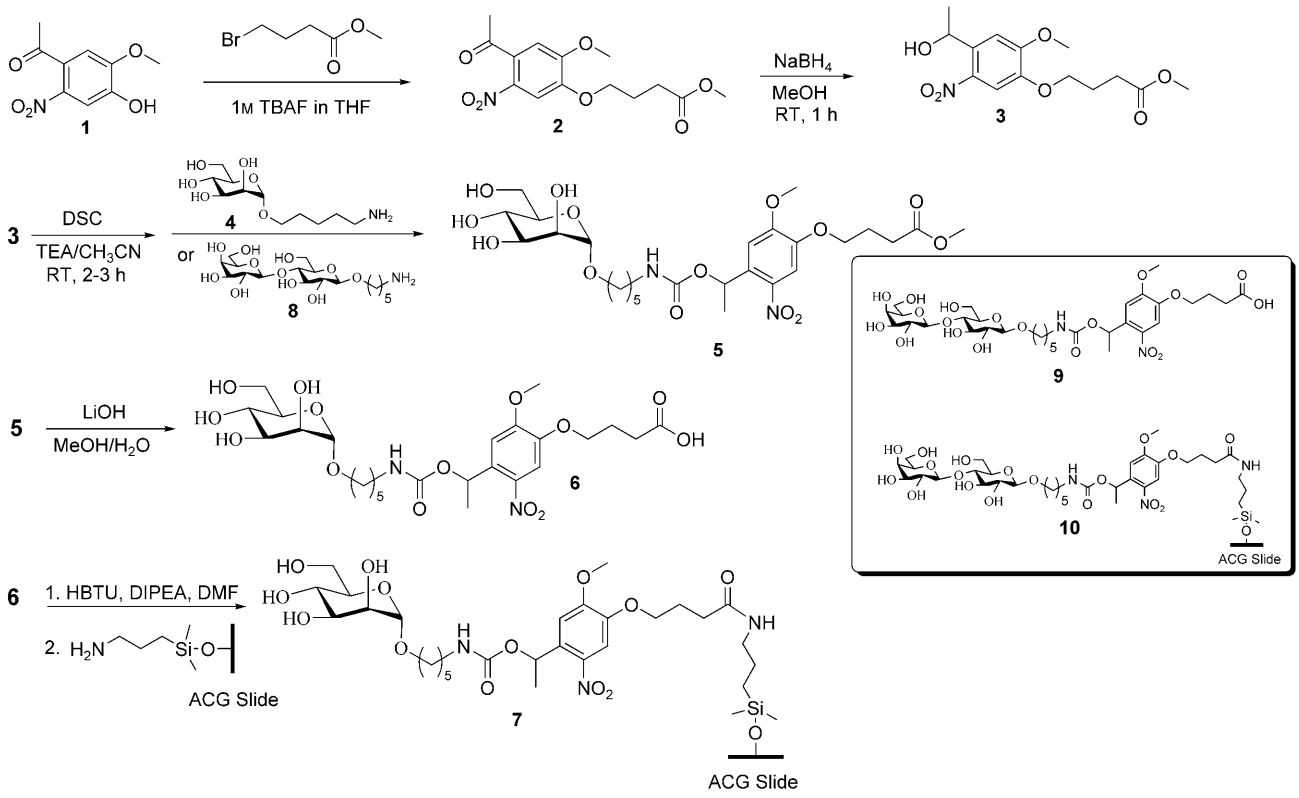

Scheme 2. Synthesis of mannose–ACG and lactose–ACG with a photocleavable linker. DIPEA = *N*,*N*-diisopropylethylamine, DSC = *N*,*N*′-disuccinimidyl carbonate, HBTU = 2-(1-benzotriazol-1-yl)-1,1,3,3-tetramethyluronium hexafluorophosphate, TBAF = tetra-*n*-butylammonium fluoride, TEA = triethylamine.

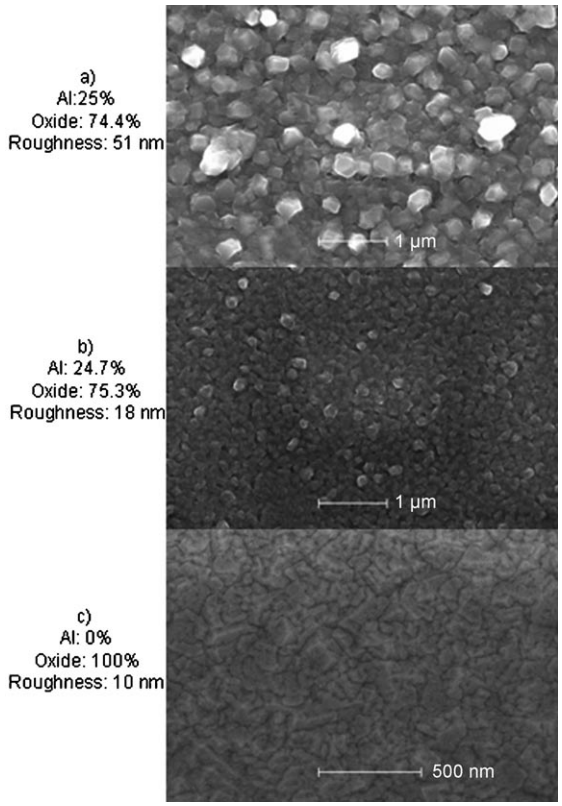

Figure 1. SEM images showing surface morphology, composition, and roughness of NAO/ACG slides obtained by a) cathode arc evaporation and b) magnetron sputtering, and c) an AAO/ACG slide obtained by thermal coating followed by electrochemical surface anodization.

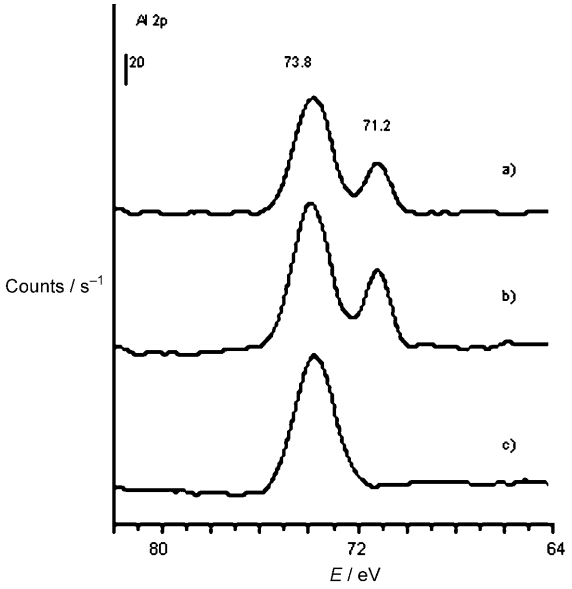

Figure 2. XPS spectra of the surface composition of a) an NAO/ACG slide obtained by cathode arc evaporation, b) an NAO/ACG slide obtained by magnetron sputtering, and c) an AAO/ACG slide obtained by thermal coating followed by surface anodization. The binding energy for C(1s) at 284.5 eV and O(1s) at 531 eV were used to calibrate the binding energy of these spectra.

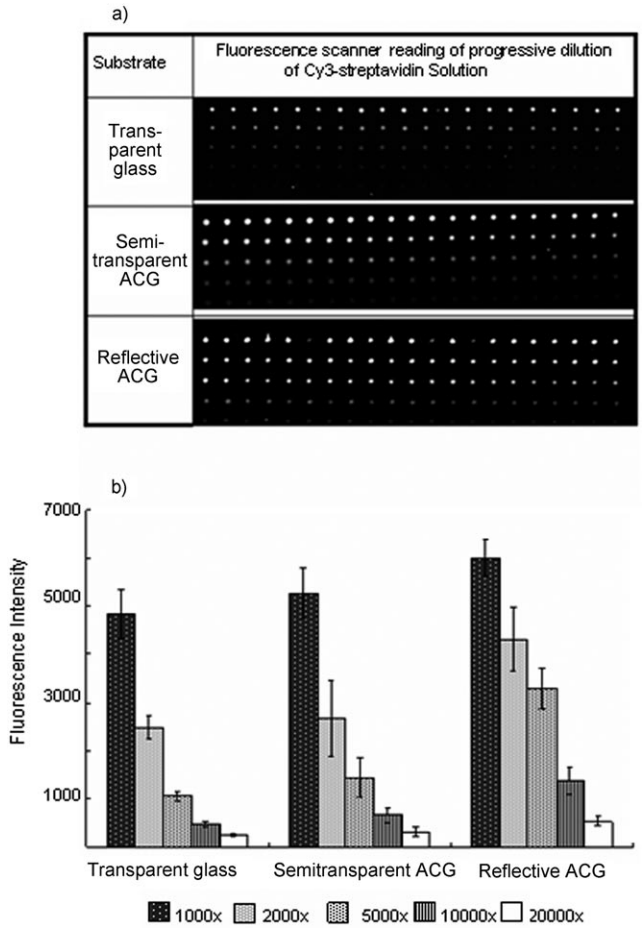

Figure 3. Optical properties of the micro glass slide, the semitransparent ACG slide, and the totally reflective (nontransparent) ACG slide. a) A series of Cy3–streptavidin solutions of 1 mg mL^{-1} original concentration diluted 1000, 2000, 5000, 10000, and 20000 times was spotted on each of these slides, air-dried, and analyzed with an arrayWoRx fluorescence spectrometer. A light source of wavelength 540 nm was provided by the instrument. Fluorescence of wavelength 595 nm was emitted from the slide surface and detected by the detector. The scanner detected the fluorescence only up to 5000 times dilution for the transparent micro glass slide, but up to 10000 and 20000 times dilution, respectively, for the semitransparent ACG slide and the totally reflective ACG slide, in which the thickness of the coated aluminium varied from a few nanometers in the former to greater than 100 nm in the latter. b) The actual calculated fluorescence intensity for each substrate.

A series of progressively diluted streptavidin-Cy3 solutions was arrayed on these slides, dried, and analyzed by an arrayWoRx fluorescence spectrometer. The wavelength for Cy3 excitation is 540 nm, and the fluorescence peak at 595 nm was measured by the detector. As shown in Figure 3, the detection sensitivity for the nontransparent (or reflective) ACG slide is the highest among all slides prepared.

Surface Activation

In the screening experiments, plasma of oxygen, argon, and mixed gases of oxygen and argon were tested for slide-surface activation. The residues (CO, CO_2, and H_2O) were removed under vacuum. It is the removal of this surface con-

CHEMISTRY
AN ASIAN JOURNAL

tamination that contributed to the success of grafting the desired organic compounds chemically. The surface was gauged with an attenuated total reflectance Fourier transform infrared (ATR/FTIR) spectrometer. The ATR/FTIR spectra showed Al–OH peaks at around 800–1100 cm^{-1} (Figure 4), which indicates that the surface had converted

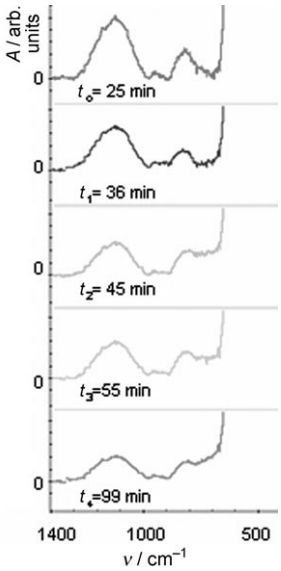

Figure 4. ATR/FTIR spectra of Al–OH on an ACG slide. The Al–OH peak intensity in the 800–1100 cm^{-1} region decreased significantly from 25 to 99 min after plasma treatment.

into Al–OH after the surface-cleaning process.[13–14] The idea behind the plasma treatment is to use just enough plasma energy to clean and "tickle" the surface of the ACG slide to remove the organic contamination but still hold the alumina layer without etching the underlying surface. The activation process was successfully completed by using a mere 6.8 W (at 680 V) of energy for 10 min under a gas-flow pressure of 270–300 mTorr. Argon plasma turned out to be the most effective for grafting sugar derivatives, as observed in later experiments.

The hydrophilic surface after plasma treatment gradually became hydrophobic, possibly because the oxide layer on the surface reformed. Disappearance of Al–OH from the substrate surface was traced by ATR/FTIR spectroscopy. The Al–OH peak intensity[13] in the 800–1100 cm^{-1} region decreased significantly over a matter of hours (Figure 4). Therefore, it was necessary to treat the ACG slides with 3-aminopropyldimethylethoxysilane (APDMES) immediately after plasma treatment. This activated ACG surface was used to immobilize the sugar derivative of mannose and lactose with a PCL in the next step of the reaction.

As shown in Figure 5, the water contact angle on the surface changed during surface activation. Therefore, measurement of the contact angle can be used as a quick check of the completion of the activation process. Substrates with a high surface roughness tend to give smaller contact angles.

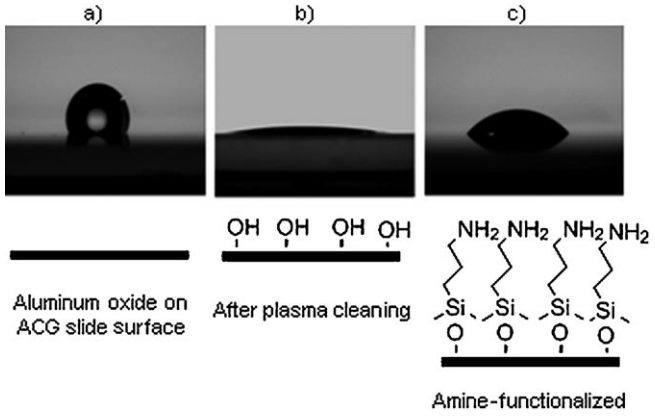

Figure 5. Typical changes in water contact angle for ACG slides that were a) solvent-cleaned, b) treated with plasma, and c) activated with 3-aminopropyldimethylethoxysilane. These samples were made and measured as an example with the nontransparent magnetron-sputtered ACG slide.

Mannose with PCL Immobilized on the Activated Surface of the ACG Slide

As shown in Scheme 2, compound **6**, which has a carboxy functional group, was synthesized. A solution[15] of HBTU and compound **6** was manually spotted and microarrayed on the activated surface of the ACG slide. Amide formation on the surface of the ACG slide took place overnight at room temperature. All salt residues, as well as unbound mannose derivative, were washed away thoroughly with methanol and deionized water. After all these preparations, the substance was ready for mass identification and protein-binding evaluation.

Mass Spectrometric Analysis of the Sugar Derivative Grafted on the ACG Slides

We learned that the matrix-free porous silicon surfaces (DIOS) produced molecular-ion peaks with negligible sample fragmentation. The ACG slide dimensions ($75.5 \times 25.4 \times 1$ mm^3) fit well in the ultraflex mass spectrometry instrument; slides at each step of the treatment were analyzed, as shown in Figure 6 (see also Scheme 3).

Figure 6a and b shows the MS data for the early experiments on a pure aluminum plate and ACG slide, whereby the mannose peak intensities were relatively low. Figure 6c shows the MS data of the ACG slide produced by cathode arc evaporation, for which the surface-activation conditions were optimized and the peak intensity of the mannose derivative was high. Although the substrates gave large background peaks at m/z 415 and 451 (Figure 6a and c), the molecular weight of the mannose derivative (265) was detected quite easily by its adducts with proton (m/z 266), lithium (m/z 272), sodium (m/z 288), and sometimes potassium (m/z 304) ions.

According to Heijnsbergen et al.,[16] under high vacuum, UV excimer laser vaporizes aluminum oxide clusters to the gas phase; ultraviolet photon ionization produces sparse

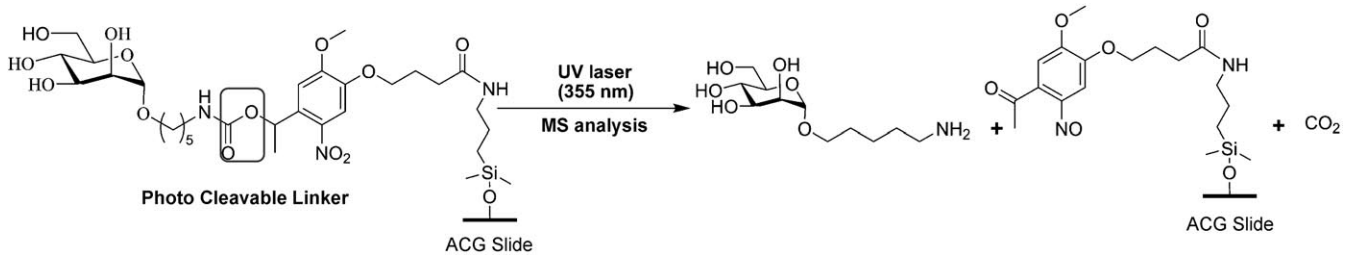

Scheme 3. Selective bond cleavage and detection of the sugar (mannose) derivative by ultraflex mass spectrometry.

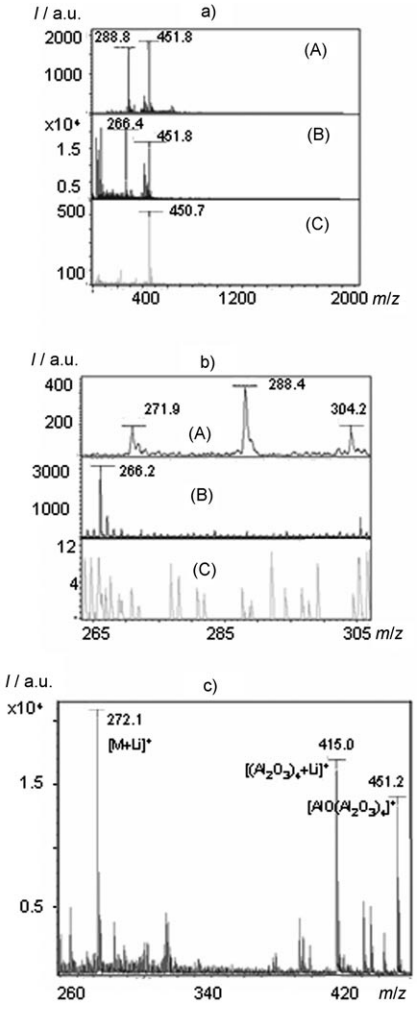

Figure 6. a) Ultraflex TOF mass spectra of mannose with PCL grafted on A) a 99.999% pure aluminum plate (1 mm thick) and B) an ACG slide formed by cathode arc evaporation. C) The background signal for cathode arc evaporation of the ACG slide. b) Ultraflex TOF mass spectra of a) at the *m*/*z* region of interest. c) TOF mass spectrum of mannose with PCL grafted on an ACG slide formed by cathode arc evaporation at the *m*/*z* region of interest.

mass spectra with relatively light aluminum oxide clusters. The majority of the oxide clusters in the gas phase under vacuum consisted of $AlO(Al_2O_3)_n$, even though the aluminum oxide clusters could exist in many different forms.[16] In Figure 6a and c, the large background peaks that occurred at *m*/*z* 451 and 415 are speculated to belong to the oxide clusters $[(Al_2O_3)_4+Li]^+$ and $[AlO(Al_2O_3)_4]^+$.

Semiquantitative Comparison of the Content of Mannose with Its Protein-Binding Capability

The optimization of the plasma gas treatment on the same type of ACG slide was evaluated by the fluorescence intensity of the immobilized sugar–protein binding. Figure 7 was obtained by selecting the type of gas used for plasma cleaning. ACG slides produced by cathode arc evaporation were exposed to oxygen, argon, or a mixture of oxygen and argon plasma gases prior to aminosilane grafting. A 10×10 block (100 spots) of the mannose derivative (sugar complex solution, 160 mM) was microarrayed onto the substrate surfaces. The sugar complex solution was also manually spotted on each of these slides (1 μL per spot) specifically for mass identification. Therefore, these slides were analyzed first by mass spectrometry and then subjected to biotinylated ConA binding followed by Cy3-tagged streptavidin detection. Figure 7a–d shows the protein-binding assays of the arrayed slides; Figure 7f shows the fluorescence intensities of substrates versus those of the commercially available glass slide. The intensity difference shown in Figure 3 demonstrates the absolute effect of the physical properties of the substrate. The intensity difference in Figure 7f resulted from the effects of both the physical properties of the specific substrates and the binding-site architectures between the immobilized sugar and its binding proteins. Both sets of data indicate that argon plasma treatment of the ACG slide surface produced the best substrate for mannose grafting, hence the mannose–protein binding.

A semiquantitative comparison of the content of the immobilized mannose and the mannose–protein binding capability are given in Figures 8 and 9. Two different types of slide substrates were used for immobilizing mannose with the built-in PCL, that is, the NH_2 functionalized glass slide and the APDMES-activated NH_2–ACG slides that were thermally coated with aluminum followed by surface-anodization treatment. The mannose–ACG slide was first subjected to MS analysis for molecular-weight identification and then to protein-binding evaluation along with the mannose–

CHEMISTRY
AN ASIAN JOURNAL

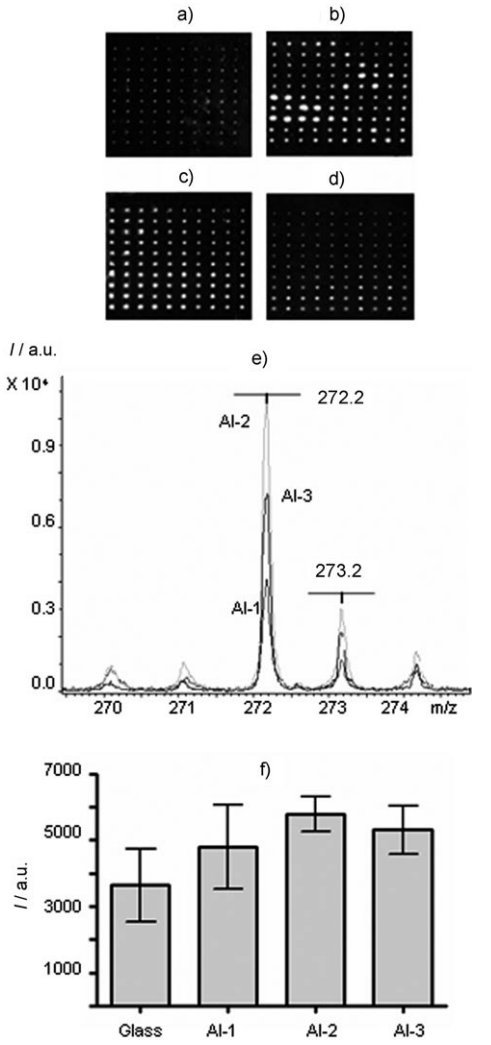

Figure 7. Protein-binding assays of ACG slides formed by cathode arc evaporation upon treatment with a) oxygen plasma (Al-1), b) argon plasma (Al-2), and c) a mixture of oxygen and argon plasma (Al-3) prior to APDMES grafting. d) Protein-binding assay of the commercially available NH_2–glass slide from Corning Glass (#40004). e) Signal intensities from MALDI mass spectra for the mass identification of sugar. The maximum-intensity spectra (70% fluence) observed from each substance was used to create this graph. f) Fluorescence intensities of a)–d) with standard errors calculated with an arrayWoRx fluorescence spectrometer. The array was made in four blocks per slide with 10×10 (100) spots per block of the same aqueous solution of sugar complex. Only the best block from each slide was chosen (as shown in b)–d)); large spots among the best blocks were eliminated for fluorescence-intensity calculations.

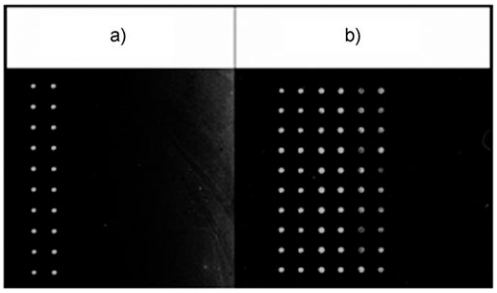

Figure 8. Fluorescence-tagged protein-binding assay of mannose immobilized on a) a glass slide and b) an ACG slide. The NH_2-functionalized glass slide was purchased from Corning Glass (#40004). The ACG slide was thermally coated with pure aluminum and then electrochemically anodized. The array was made in a block of 10×6 (60) spots. The solution of sugar–HBTU complex (156 mM) was prepared to 100 and 10000 times dilution. Each solution was spotted in two columns (20 spots) in the block for grafting. Substrate a) shows fluorescence only in the first two columns (the solution of sugar complex), but substrate b) shows signals up to the sixth column (10000 times dilution of the starting solution of sugar complex).

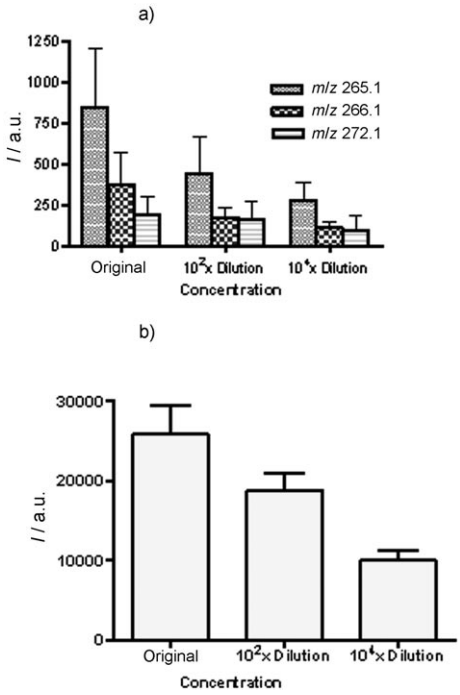

Figure 9. Comparison of the peak intensities of the ultraflex TOF mass spectra of mannose with PCL grafted on ACG slides with the fluorescence intensities of mannose–protein-bound ACG slide formed by thermal coating followed by electrochemical anodization on the slide surface. The concentration of the mannose solution varied from 156 mM to 102 (1.56 mM) and 104 times dilution (15.6 nM). a) Average peak intensities of mannose mass spectrometric adducts obtained at m/z 265.1 $[M]^+$, 266.1 $[M+1]^+$, and 272.1 $[M+Li]^+$. b) Corresponding fluorescence intensities of the same mannose–ACG slide sample obtained from the fluorescence-tagged protein-binding assay.

glass slide. Figure 8 shows the protein-binding data resulting from the two different types of slide substrates. It clearly indicates that the mannose–ACG slide (Figure 8b) showed higher fluorescence of Cy3 with a better sensitivity than the glass slide (Figure 8a). The fluorescence intensity from the ACG slide was calculated and is given in Figure 9b.

The differences in fluorescence intensity in Figure 8 were caused by the difference in physical properties of the slide substrates and the difference in the degree of mannose–ConA and Cy3–streptavidin binding. This difference in turn, implies a variation in the grafting density of mannose on the substrate surface. A recent report indicated[22] that the interaction between ConA and mannose becomes weak when the density of mannose on the substrate surface is about

100 Å apart,[17] thus reflecting the degree of polyvalent interaction.

MS analysis of the same mannose–ACG slide (Figure 8b) revealed the parent peak (*m*/*z* 265) as well as the proton (*m*/*z* 266) and lithium (*m*/*z* 272) adducts. In analyzing this slide, each manually spotted (in the series of dilutions) sample was measured six times with 500 shots per measurement. The average peak intensity with standard deviation is given in Figure 9a, which demonstrates that MS could still identify the sugar, even when the concentration of the solution for grafting was diluted to 15.6 nM. The signal intensities measured by MS (Figure 9a) are further compared to the fluorescence intensities shown in Figure 9b. The descending trends of these two different measurements are similar. Apparently, the quantity of immobilized sugar reflects its protein-binding capability.

Utility of ACG Slides on Carbohydrate Microarrays

By using the synthetic route in Scheme 2, lactose with PCL was also immobilized on an ACG slide (Figure 10a). As seen in the MS analysis of this sample (Figure 10b), the interference occurred resulting from the sparse aluminum oxide peaks at 415 and 451. However, the molecular weight of the lactose derivative (*m*/*z* 427) could still be clearly identified by its adducts with proton (*m*/*z* 428), sodium (*m*/*z* 450), and potassium (*m*/*z* 466) ions.

For further utilization of this newly fabricated substrate, the NH_2–ACG surface was modified through conversion into NHS–ACG by treatment with disuccinimidyl suberate (DSS) in DMF and diisopropylethylamine. With glass slides as reference, a Globo H derivative with an amine functional group was arrayed on the NHS–ACG slide (Figure 10c) and subjected to VK9 (a mouse IgG anti-Globo H monoclonal antibody) protein-binding evaluation.[4] The results in Figure 10d and e indicate that the ACG slide shows the highest fluorescence intensity among all three samples.

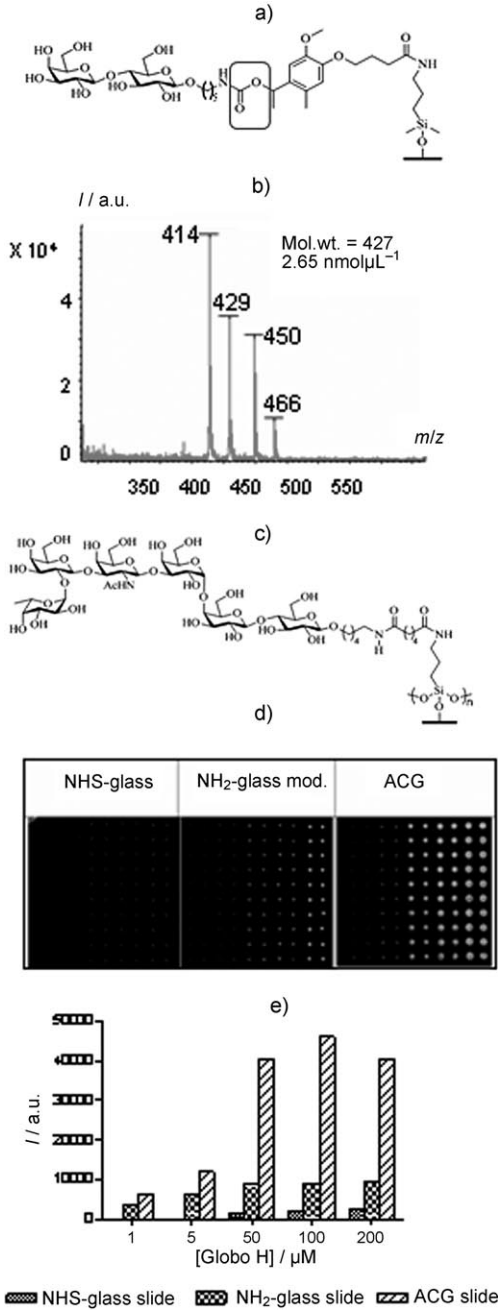

Figure 10. a) Lactose–ACG slide with PCL. b) Ultraflex TOF mass spectra obtained from the lactose–ACG slide with PCL. c) Globo H–ACG slide with no PCL. d) Fluorescence-tagged protein-binding assay of Globo H immobilized on NHS–glass slide, NH_2-modified glass slide (Corning #40004), and NHS–ACG slide. e) Corresponding fluorescence intensities calculated from d) with a GenePix 4000 fluorescence scanner.

Factors Affecting Fluorescence Intensity

Substrate Property and Surface Morphology

The optical properties of substrates apparently affect the fluorescence intensity. Fluorescence (Cy3) is the sole light source in a protein-binding assay. Glass as well as porous silicon both pass and reflect light to different extents. On the contrary, aluminium-coated glass can be fabricated such that it becomes completely nontransparent and minimizes the "waste" of light provided by the light source.

The surface morphology of the substrate could affect the grafting density in immobilizing sugars. The NAO surface showed only 75% oxide content. On the contrary, the AAO surface contains 100% aluminum oxide, thus providing a stable surface and leading to a steady immobilizing density of the final slide for assay.

Substrate stability may also be affected by the way in which the surface is chemically treated. An example is the surface with cross-linked amines versus that with a monolayer of amine functional groups, both of which were made by activating the ACG slide with either 3-aminopropyltrieth-oxysilane (APTES) or 3-aminopropyldimethylethoxysilane (APDMES). Various chemical treatments of the ACG slide surface are under investigation.

CHEMISTRY
AN ASIAN JOURNAL

Binding-Site Architectures/Interactions of Proteins with Sugars Immobilized on the Substrate Surface

Under our experimental conditions, both concanavalin A and streptavidin exist as tetramers of their quaternary structures.[18–22] The ratio of the dimensions of mannose to ConA is about 1:400 (corresponding to their molecular weight of 265 vs. 104 kDa). Owing to the geometric constraint, only two binding sites per tetramer of biotinylated ConA are available for mannose binding on the surface. On the high-density mannose array surface, each ConA tetramer would bind two molecules of mannose, and the two mannose molecules would probably be grafted on the surface not too far away from each other. As the chain length of the mannose derivative increases, the grafted mannose becomes further away from the substrate, and a high degree of randomness of the interaction could occur when both the grafting density and the amount of immobilized sugar–protein binding increase. Furthermore, we allowed the flexible docking of the streptavidin–Cy3 complex to biotinylated ConA. A similar geometric restriction can also be illustrated for Globo H, IgG monoclonal antibody VK9 (from mouse), and its goat anti-mouse IgG protein. The binding-site architecture between sugar and proteins could affect the density of the fluorescence-tagged protein and, thus, the fluorescence intensity in the sugar–protein-binding assay.

One purpose of studying the surface immobilization of sugars is to mimic the ligand interactions that occur on the cell surface of biological entities,[4,23,24] for example, the existence and overexpression of the sugar antigen Globo H on the surfaces of normal and malignant cells. The sugar antigens, when overly populated on the cell surfaces, could result in massive polyvalent carbohydrate–protein interactions and greatly impact the provided biological function of the living entities. This study provides a more precise quantitative measurement and comparison of such a biological system.

Conclusions

Newly fabricated aluminum-coated glass (ACG) slides have been developed for immobilizing sugars. Mannose and lactose with a built-in photocleavable linker immobilized on the ACG slide surfaces were subjected to MALDI MS analysis to characterize the molecular weight of the immobilized sugars. A proportional correlation was observed between the quantity of mannose (m/z) and the fluorescence intensity of its protein binding. In protein-binding assays of mannose–ACG and Globo H–ACG slides, we observed higher fluorescence intensity and sensitivity than with glass slides, perhaps due to the material properties, surface morphologies, and binding-site architectures between proteins and the immobilized sugars on the slide surfaces.

Experimental Section

Substrate Materials

Micro glass slides ($75.5\times25.4\times1$ mm^3) were cleaned in piranha solution, a mixture of concentrated H_2SO_4 and 30% H_2O_2 (70:30 *v*/*v*), at 120 °C for 30 min, rinsed with plenty of deionized water until pH 7, and purge-dried with high-quality nitrogen gas. The high-purity aluminum targets (99.999% pure) were obtained from Summit-Tech Resource Corp. (Hsin-Chu, Taiwan). These raw materials were provided to vendors Cheng-Jen Corp. (Kao-Hsiung, Taiwan) and Yujay-Tech Corp. (Chin-Ju, Taiwan) for the fabrication of ACG slides by using different coating techniques such as magnetron sputtering, cathode arc evaporation, and thermal evaporation.[26] The fabricated ACG slides were either used directly or anodized with a DC current at 20 V (Keithley 2400 Model) at 4 °C in 0.3 M aqueous oxalic acid for 60–90 s.[26] The surface properties of the fabricated ACG slides are shown in Figure 1. The surfaces were sputtered with gold and examined by SEM (FEI XL30 SFEG, FEI Company). The surface roughness and thickness of the aluminum coating were measured by AFM (Dimension 3100 Veeco Instruments, Inc.). The surface compositions of these slides were analyzed by XPS by using an Omicron ESCA spectrometer with a monochromatic $Al_{K\alpha}$ X-ray (1486.6 eV) source under ultra-high vacuum (1×10^{-10} Torr). All spectra were calibrated by the carbon 1s spectrum at 284.5 eV and the oxygen 1s spectrum at 532 eV.

Fabrication of NH_2–ACG Slides

The ACG slide was washed with acetone and water consecutively on a multishaker (FMS2 FINEPCR) for 2–3 min, purge-dried with high-purity nitrogen gas, and further dried in an oven at 100 °C for 10–15 min. Surface activation was conducted by a plasma cleaner (Harrick PDC 32 G, 200–600 mTorr) with oxygen, argon, or mixed gases at room temperature for 10 min. Immediately after plasma treatment, APDMES (0.8 mL) was placed evenly on the surface (in bulk), which was covered with a sealed petri dish and heated directly on a hot plate at 65 °C for 40 min–1 h. When the reaction was completed, the sample slide was rinsed thoroughly, sonicated in methanol for 3 min (20% power), and purge-dried with high-purity nitrogen gas. The surface with aminosilane-grafted substrate was used for amide-linkage formation in situ with the mannose derivative compound **6** and HBTU. The commercial NH_2–glass slides (#40004 from Corning Inc.) were used for comparison of protein binding.

Fabrication of NHS–ACG Slides

ACG slides coated by thermal evaporation were further anodized in 0.3 M oxalic acid for 90 s, rinsed with deionized water, and activated by argon plasma as usual. Without any contamination, the slide was assembled in a designed teflon sealed, heat-transferable reaction cell, and APTES (1 mL, bulk) was immediately added to the cell. The teflon cell was covered with a glass plate. Under moisture-free conditions, the cell was heated at 65 °C for 30 min and rinsed thoroughly with methylene chloride and methanol. The slides were then purge-dried with nitrogen gas. Beforehand, a saturated solution of DSS (0.5 g; CAS #68528-80-30) in DMF (4 mL) and diisopropylethylamine (220 μL) was prepared. A portion (1.33 mL) of this saturated solution was added to each reaction cell. The NHS–ACG slide was formed within 3 h with constant swirling at room temperature. The slide was rinsed thoroughly with ethyl acetate and purge-dried with high-quality nitrogen gas. After the teflon cell was dried and disassembled, the slide was ready for Globo H–NH_2 microarray.

Reference-Controlled NHS–Glass Slides

NHS–glass slides (from SCHOTT, North America) were used directly. The NH_2–glass slide (#40004 from Corning, Inc.) was modified by using the same preparation method for the NHS–ACG slide. The slide was assembled in a designed teflon sealed, heat-transferable reaction cell. A portion (1.33 mL) of saturated DSS solution was added for reaction with the NH_2–glass surface. After constant swirling at room temperature for 3 h, the slide was rinsed thoroughly with ethyl acetate and purge-dried with high-quality nitrogen gas. After the teflon cell was dried and disassembled, the slides were ready for Globo H–NH_2 microarray.

Chemical Materials

All chemicals employed in the synthesis of **6** were purchased from Aldrich or the specified individual chemical companies and used without any further purification.

Syntheses

5: As shown in Scheme 2, the intermediate product prepared from **3** had to be used immediately. Therefore, this step was carried out prior to the reaction with **4**[25] (similarly with **8**). Compound **1** was prepared by using the method reported previously.

2: In a 100-mL round-bottomed flask, a solution (13.3 mL) of TBAF (1 M, 13.3 mmol) in THF was added to a mixture of **1** (2.0 g, 9.48 mmol) and methyl-4-bromobutyrate (1.96 g, 10.8 mmol) at room temperature. The solution was kept stirring at room temperature for 12 h, and the solvent was evaporated under reduced pressure. The residue was extracted with methylene chloride and saturated aqueous sodium bicarbonate. The product was collected by evaporating the organic layer and purified by silica-gel column chromatography (EtOAc/hexane = 4:1) to afford **2** (2.9 g, 98%). ^{1}H NMR (600 MHz, $CDCl_3$): δ = 7.59 (s, 1H), 6.73 (s, 1H), 4.13 (t, J = 6.2 Hz, 2H), 3.93 (s, 3H), 3.69 (d, J = 9.5 Hz, 3H), 2.54 (t, J = 7.1 Hz, 2H), 2.49 (q, J = 7.2 Hz, 3H), 2.20–2.13 ppm (m, 2H); ^{13}C NMR (150 MHz, $CDCl_3$): δ = 177.9, 173.2, 128.8, 117.9, 111.1, 109.1, 108.3, 106.8, 68.5, 56.5, 51.9, 32.9, 27.9, 24.3 ppm; HRMS (ESI-TOF): m/z calcd for $C_{14}H_{17}NO_7$: 311.1005 $[M+Na]^+$; found: 334.0915.

3: Sodium borohydride (0.35 g, 9.25 mmol) was added to a solution of **2** (2.9 g, 10.9 mmol) in methanol (37 mL) at 0 °C. The ice bath was then removed, and the reaction mixture was stirred at room temperature for 1 h. The solvent was extracted under reduced pressure, and the residue was extracted with water and ethyl acetate. The product was collected by evaporating the organic layer and purified by silica-gel column chromatography (EtOAc/hexane = 4:1) to afford **3** (2.0 g, 68%). ^{1}H NMR (600 MHz, CD_3OD): δ = 7.58 (s, 1H), 7.39 (s, 1H), 5.46 (q, J = 6.2 Hz, 1H), 4.10 (t, J = 6.2 Hz, 2H), 3.96 (s, 3H), 3.35 (s, 3H), 2.51 (t, J = 7.3 Hz, 2H), 2.10 (q, J = 6.4 Hz, 2H), 1.47 ppm (d, J = 6.3 Hz, 3H); ^{13}C NMR (150 MHz, CD_3OD): δ = 175.5, 155.6, 148.3, 140.3, 139.1, 110.2, 110.4, 69.6, 66.4, 56.8, 52.3, 31.4, 25.7, 25.3 ppm; HRMS (ESI-TOF): m/z calcd for $C_{14}H_{19}NO_7$: 313.3032 $[M+Na]^+$; found: 336.1073.

5: Compound **3** (0.60 g, 1.9 mmol) was dissolved in acetonitrile (12 mL) in a 50-mL round-bottomed flask. DSC (0.73 g, 2.72 mmol) and triethylamine (0.57 g, 5.6 mmol) were added at room temperature. The solution was stirred at room temperature for 2.5 h. The solvent was evaporated, and saturated aqueous sodium bicarbonate (10 mL) was added to remove the excess reagent. The product was extracted with ethylene chloride (10 mL) three times, and the organic layer was collected. After the solvent was evaporated, the residue was dissolved in dry DMF (11.2 mL) in a 50-mL round-bottomed flask. Compound **4** (0.33 g, 1.24 mmol) and DIPEA were added to the solution at room temperature. The solution was stirred overnight at room temperature and checked for completion of the reaction by TLC with MeOH/CH_2Cl_2 (1:5). After removal of the solvent, the purified product **5** (260 mg, 35%) was obtained by silica-gel column chromatography. ^{1}H NMR (600 MHz, $CDCl_3$): δ = 7.50 (s, 1H), 6.97 (s, 1H), 6.26 (q, J = 6.2 Hz, 1H), 5.32 (dd, J = 5.3 Hz, J = 4.2 Hz, 1H), 4.71 (br s, 1H), 4.04 (t, J = 6.1 Hz, 2H), 3.88 (s, 3H), 3.88 (dd, J = 10.2 Hz, J = 5.4 Hz, 1H), 3.86 (br s, 1H), 3.82 (br s, 1H), 3.73 (br s, 1H), 3.68 (dd, J = 9.9 Hz, J = 6.0 Hz, 1H), 3.62 (s, 3H), 3.54 (dd, J = 8.3 Hz, J = 5.4 Hz, 1H), 3.41 (dd, J = 9.2 Hz, J = 5.0 Hz, 1H), 3.30 (dd, J = 8.4 Hz, J = 5.4 Hz, 1H), 3.05 (dd, J = 6.3 Hz, J = 5.0 Hz, 1H), 2.99 (dd, J = 6.3 Hz, J = 4.2 Hz, 1H), 2.49 (t, J = 7.2 Hz, 2H), 2.11 (q, J = 6.7 Hz, 2H), 1.51 (dd, J = 6.4 Hz, J = 2.1 Hz, 3H), 1.48 (br s, 2H), 1.40 (q, J = 7.2 Hz, 2H), 1.30–1.21 ppm (m, 2H); ^{13}C NMR (150 MHz, $CDCl_3$): δ = 173.6, 173.2, 155.7, 154.2, 147.1, 139.6, 109.1, 108.3, 100.1, 72.3, 71.7, 71.1, 68.8, 68.3, 67.6, 66.5, 61.1, 56.5, 51.9, 41.0, 30.5, 29.8, 29.0, 24.3, 23.5, 22.3 ppm; HRMS (ESI-TOF): m/z calcd for $C_{26}H_{40}N_2O_{14}$: 604.2408 $[M+Na]^+$; found: 627.2375.

6: At 0 °C, LiOH (36.0 mg, 0.86 mmol) was added to a solution of **5** (0.26 g, 0.43 mmol) in MeOH/H_2O (4:1, 3.6 mL). The reaction was conducted at room temperature for approximately 6 h until completion of the reaction. Aqueous HCl (1 N) was added to neutralize the mixture to pH 7, and the solvent was evaporated under vacuum. The residue was purified by silica-gel column chromatography to afford **6** (0.2 g, 79%). ^{1}H NMR (600 MHz, CD_3OD): δ = 7.62 (s, 1H), 7.16 (s, 1H), 6.25 (d, J = 6.4 Hz, 1H), 4.71 (d, J = 1.9 Hz, 1H), 4.08 (t, J = 6.4 Hz, 2H), 3.95 (s, 3H), 3.82 (dd, J = 2.2, 4.4 Hz, 1H), 3.76 (dd, J = 4.5 Hz J = 1.5 Hz, 1H), 3.72 (dd, J = 3.0 Hz, J = 2.1 Hz, 1H), 3.71 (dd, J = 2.2, 4.0 Hz, 1H), 3.69 (br s, 1H), 3.58 (t, J = 9.6 Hz, 1H), 3.50 (br s, 1H), 3.41–3.35 (m, 1H), 3.05 (t, J = 6.9 Hz, 2H), 2.44 (t, J = 7.4 Hz, 2H), 2.10 (q, J = 6.9 Hz, 2H), 1.58 (d, J = 3.3 Hz, 3H), 1.58 (q, J = 6.5 Hz, 2H), 1.48 (q, J = 7.0 Hz, 2H), 1.36 ppm (q, J = 7.6 Hz, 2H); ^{13}C NMR (150 MHz, CD_3OD): δ = 179.7, 172.6, 158.1, 155.8, 141.1, 135.4, 110.1, 109.4, 101.7, 74.8, 72.7, 72.4, 70.0, 69.8, 68.7, 68.5, 63.1, 57.0, 41.7, 33.4, 30.5, 30.4, 26.6, 24.7, 22.6 ppm; HRMS (ESI-TOF): m/z calcd for $C_{25}H_{38}N_2O_{14}$: 590.2323 $[M+Na]^+$; found: 613.2224.

Immobilization of mannose with a PCL onto the NH_2–ACG slides[15] (**7**): Mannose derivative **6** (11.8 mg, 0.02 mmol) was dissolved in DMF (118 μL). With constant stirring, HBTU (11.4 mg, 0.03 mmol) and DIPEA (7 μL, 0.042 mmol) were added consecutively to the mixture. The complex formed within an hour with a change in the solution from brown to reddish orange. The freshly prepared sugar solution was spotted manually (for MS analysis) and also microarrayed on the activated ACG slides. Microarray was constructed with a BioDot AD3200 instrument (Agilent Technology) by robotic pin (Array It, Stealth Micro Spotting Pin, SMP4) deposition of approximately 1.1 nL of the sugar solution per spot of the arrays. Four or five blocks (9 mm separation between blocks) with 10×10 (or 10×6) spots per block (100 or 60 spots, separated by 0.80 mm) were printed on each slide, and the slides were left overnight in a sealed petri dish saturated with diisopropylethylamine vapor. On the next day, the slides were rinsed with plenty of methanol and purge-dried gently with high-purity nitrogen gas. The prepared sample **7** was stored in the dark prior to MS analysis and protein-binding study.

Immobilization of lactose with a PCL onto the NH_2–ACG slides:[15] Lactose derivative **9** (0.08 mmol) was dissolved in DMF (3 mL). With constant stirring, HBTU (40 mg, 0.1 mmol) and DIPEA (27 μL, 0.16 mmol) were added to form the mixture of sugar complex. The complex was formed within an hour with a change in the solution from brown to reddish orange. The freshly prepared sugar solution was manually spotted and left overnight for amide bond formation in situ. On the next day, the slides were rinsed with plenty of methanol and purge-dried gently with high-purity nitrogen gas. The prepared sample **10** was stored in the dark prior to MS analysis.

Immobilization of Globo H with an amine functional group onto the NHS–ACG slides: Globo H solutions (50 μL) of various concentrations (200, 100, 50, 5, and 1 μM) were placed in a solvent-resistant PP microarray tray. A BioDot AD3200 instrument was used to microarray these sugar solutions. Four blocks of 100 dots per block (10×10; 20 dots for each concentration of solution) of Globo H were arrayed on an NHS–glass slide (SCHOTT), an NHS–glass slide modified from an NH_2-functionalized glass slide (Corning #40004), and an NHS–ACG slide under 80% controlled relative humidity. These slides were left overnight in the array chamber and used for protein-binding analysis the next day.

Mass Spectrometry

The immobilized slide was analyzed with a Bruker Ultraflex MALDI-TOF mass spectrometer equipped with a nitrogen pulsed laser (355 nm). Each data point was collected at the average of 500–1000 shots of the laser beam, and the laser fluence was applied at 40–95%, with the best results obtained mostly at 50–80%. A standard aqueous solution of mannose–NH_2 was manually deposited on a defined area of the ACG slide and used to calibrate the data obtained from the immobilized sugars on the same slide substrate. For quantitative comparison of the grafted mannose derivatives at different concentrations, all analyses were made at a single measurement of 500 shots at 80% fluence. The variation in average peak intensity with S/N ratio was plotted.

Protein-Binding Assay

Mannose–protein-binding assay of immobilized mannose with biotinylated ConA and Cy3-tagged streptavidin: The same slide used for MS analysis was washed again with distilled water under mild sonication and then rinsed with PBS (phosphate-buffered saline) buffer. Biotin-labeled ConA (Invitrogen C 21420) was diluted 500–1000 times in PBST buffer (PBS with 0.05 % Tween 20). The protein solution (50 μL) was applied to each array substrate and incubated in a Whatman 16-pad incubation chamber. These slides were wrapped with foil and incubated for 1 h in a shaker at room temperature. After the incubation, the slides were washed three times with PBST buffer. Streptavidin–Cy3 (Sigma S 6402) was diluted in PBS buffer 100 times, and the slides were covered with aluminum foil and incubated again with streptavidin–Cy3 for another hour. After the second incubation, the slides were washed with PBST buffer and distilled water and then purge-dried with high-quality nitrogen gas. The array pattern was analyzed in reflective mode with 540-nm laser light by using the fluorescence light scanner, ArrayWoRx, made by Applied Precision. The best block on each slide was selected for statistical fluorescence-intensity analysis.

Globo H–protein-binding assay of immobilized Globo H with monoclonal antibody VK9 (IgG) from mouse and Cy3-tagged secondary antibody: The Globo H microarray slides were blocked with aqueous ethanolamine (50 mM) to remove the unreacted NHS on the slide surface. The slides were assembled again in the reaction cell and washed with PBS buffer (pH 7.4). Next, a solution of VK9 (1 mL, 50 $\mu g\,mL^{-1}$ in each cell), the anti-Globo H monoclonal antibody (IgG) from mouse, in PBST (pH 7.4) was added to the cell. The binding experiment was conducted with constant shaking for 1 h. The slide was washed three times (with 10 min constant swirling each time) with PBST buffer (pH 7.4). Cy3-tagged goat anti-mouse IgG for VK9 was added to the cell, and the mixture was incubated with shaking in the dark for 1 h. The protein-bound slides were washed five times each with PBST buffer (pH 7.4), PBS buffer (pH 7.4), and water and then purge-dried with nitrogen gas.

Acknowledgements

We thank Dr. Yang-Yuan Chen and Dr. Shu-Hwa Chien for their help with growing the anodized ACG slides as well as the surface characterization of the slides, and Dr. Shang-Fan Lee and Mr. Kai-Wen Cheng for their help with SEM, coating-thickness, and surface-roughness measurements. We also acknowledge Mr. Hong-Young Chuang for his help with the synthesis of the lactose compound, Mr. Yung-Fung Lin for his help with the NMR spectroscopic analysis of structures and identification of the synthesized compounds, and Ms. Nien-Yeen Hsu for her help with MALDI-MS analysis.

[1] a) S. Park, I. Shin, *Angew. Chem.* **2002**, *114*, 3312–3314; *Angew. Chem. Int. Ed.* **2002**, *41*, 3180–3182; b) B. T. Houseman, M. Mrksich, *Chem. Biol.* **2002**, *9*, 443–454; c) D. Wang, S. Liu, B. J. Trummer, C. Deng, A. Wang, *Nat. Biotechnol.* **2002**, *20*, 275–281; d) S. Fukui, T. Feizi, C. Galustian, A. M. Lawson, W. Chai, *Nat. Biotechnol.* **2002**, *20*, 1011–1017; e) P.-H. Liang, C.-Y. Wu, W. A. Greenberg, C.-H. Wong, *Curr. Opin. Chem. Biol.* **2008**, *12*, 86–92, and references cited therein.

[2] J.-C. Lee, C.-Y. Wu, V. J. Apon, G. Siuzdak, C.-H. Wong, *Angew. Chem.* **2006**, *118*, 2819–2823; *Angew. Chem. Int. Ed.* **2006**, *45*, 2753–2757.

[3] O. Blixt, S. Head, T. Mondala, C. Scanlan, M. E. Huflejt, R. Alvarez, M. C. Bryan, F. Fazio, D. Calarese, J. Stevens, N. Razi, D. J. Stevens, J. J. Skehel, I. van Die, D. R. Burton, I. A. Wilson, R. Cummings, N. Bovin, C.-H. Wong, J.C. Paulson, *Proc. Natl. Acad. Sci. USA* **2004**, *101*, 17033–17038.

[4] C.-Y. Huang, D. A. Thayer, A. Y. Chang, M. D. Best, J. Hoffmann, S. Head, C.-H. Wong, *Proc. Natl. Acad. Sci. USA* **2006**, *103*, 15–20.

[5] J. Wei, J. M. Buriak, G. Siuzdak, *Nature* **1999**, *399*, 243–246.

[6] Z. Shen, J. J. Thomas, C. Averbuj, K. Broo, M. Engelhard, J. E. Crowell, M. G. Finn, G. Siuzdak, *Anal. Chem.* **2001**, *73*, 612–619.

[7] E. S. P. Bouvier, M. G. Finn, G. Siuzdak, *Anal. Chem.* **2004**, *76*, 4484–4489.

[8] K.-S. Ko, F. A. Jaipuri, N. L. Pohl, *J. Am. Chem. Soc.* **2005**, *127*, 13162–13163.

[9] R. L. Nicholson, M. L. Ladlow, D. R. Spring, *Chem. Commun.* **2007**, *38*, 3906–3908.

[10] K. Viswanathan, T. E. Long, T. C. Ward, *J. Polym Sci. Part A* **2005**, *43*, 3655–3666.

[11] B. Xia, J. Li, S.-J. Xiao, D.- J. Guo, J. Wang, Y. Pan, X.-Z. You, *Chem. Lett.* **2005**, 226–227.

[12] a) M. W. Finnis, *J. Phys. Condens. Matter* **1996**, *8*, 5811–5836; b) H. Li, A. Belkind, F. Jasen, Z. Orban, *Surf. Coat. Technol.* **1997**, *92*, 171–177.

[13] a) X.-H. Guan, Q. Liu, G.-H. Chen, C. Shang, *J. Colloid Interface Sci.* **2005**, *289*, 319–327; b) J. van den Brand, S. Van Gils, P. C. J. Beentjes, H. Terryn, J. H. W. de Wit, *Appl. Surf. Sci.* **2004**, *235*, 465–474.

[14] A. Y. Fadeev, H. Roy, M. Stephen, *Langmuir* **2002**, *18*, 7521–7529.

[15] A. Brik, C.-Y. Wu, C.-H. Wong, *Org. Biomol. Chem.* **2006**, *4*, 1446–1457.

[16] D. V. Heijnsbergen, K. Demyk, M. A. Duncan, G. Meijer, G. V. Helden, *Phys. Chem. Chem. Phys.* **2003**, *5*, 2515–2519.

[17] P.-H. Liang, S.- K. Wang, C.-H. Wong, *J. Am. Chem. Soc.* **2007**, *129*, 11177–11184.

[18] D. A. Rozwarski, B. M. Swami, C. F. Brewerm, J. C. J. Sacchettini, *J. Biol. Chem.* **1998**, *273*, 32818–32825.

[19] J. H. Nesmith, R. A. Field, *J. Biol. Chem.* **1996**, *271*, 972–976.

[20] S. Freitag, I. L. Trong, L. Klumb, P. S. Stayton, R. E. Stenkamp, *Protein Sci.* **1997**, *6*, 1157–1166.

[21] V. Chu, S. Freitag, I. L. Trong, R. E. Stenkamp P. S. Stayton, *Protein Sci.* **1998**, *7*, 848–859.

[22] S. Freitag, I. L. Trong, A. Chilkoti, L. A. Klumb, P. S. Stayton, R. E. Stenkamp, *J. Mol. Biol.* **1998**, *279*, 211–221.

[23] a) J. L. de Paz, C. Noti, P. H. Seeberger, *J. Am. Chem. Soc.* **2006**, *128*, 2766–2767; b) D. M. Ratner, P. H. Seeberger, *Curr. Pharm. Des.* **2007**, *13*, 173–183.

[24] a) L. Nimrichter, A. Cargir, M. Gortler, R. T. Altstock, A. Shtevi, O. Weisshaus, E. Fire, N. Dotan, R. L. Schnaar, *Glycobiology* **2004**, *14*, 197–203; b) M. D. Disney, P. H. Seeberger, *Chem. Biol.* **2004**, *11*, 1701–1707.

[25] Y. Gao, A. Eguchi, K. Kakehi, Y. C. Lee, *Org. Lett.* **2004**, *6*, 3457–3460.

[26] a) J. E. Mahan, *Physical Vapor Deposition of Thin Film*, Wiley Interscience, New York, **2000**; b) P. G. Sheasby, R. Pinner, *The Surface Treatment And Finishing of Aluminum And Its Alloys*, *Vol. 1*, ASM, Materials Park, Ohio, **2001**.

Received: April 2, 2008
Published online: August 5, 2008

